Inorg. Chem. **2009**, *48*, 3966−3975

Functionalization of Calix[4]arene as a Molecular Bridge To Assemble Luminescent Chemically Bonded Rare-Earth Hybrid Systems

Hai-Feng Lu,[†] Bing Yan,*[,†,‡] and Jin-Liang Liu[†]

Department of Chemistry, Tongji University, 1239 Siping Road, Shanghai 200092, People's Republic of China, and State Key Laboratory of Rare Earth Materials Chemistry and Applications, Peking University, Beijing 100871, China

Received August 4, 2008

The functional macrocyclic precursors (abbreviated as BC[4]Si and C[4]Si) derive from two kinds of calix[4]arenes, *p-tert*-butylcalix[4]arene (BC[4]) and calix[4]arene (C[4]) grafted by 3-(triethoxysilyl)propyl isocyanate (TESPIC) through base-initiated nucleophilic addition, and then three series of novel luminescent chemically bonded hybrid material systems (BC[4]Si, RE-BC[4]Si, C[4]Si, and RE-C[4]Si, where RE = Eu, Tb) with organic parts covalently linked to inorganic parts via the functionalized calix[4]arene linkages have been assembled by a sol−gel process, which is characterized by the X-ray diffraction, thermogravimetry/differential scanning calorimetry, scanning electron microscopy, and spectroscopy. It is found that the coordination of rare-earth ions has an influence on the organization and microstructure of the hybrid systems. The photoluminescent behavior (luminescence, lifetime, quantum efficiency, and energy transfer) for these chemically bonded hybrids is studied in detail. Three color luminescences are checked, blue (BC[4]Si and C[4]Si), green (Tb-BC[4]Si and Tb-C[4]Si), and red (Eu-BC[4]Si and Eu-C[4]Si), respectively, suggesting that the intramolecular energy-transfer process between the rare-earth ion and the host takes place within these molecular-based hybrids. Also, especially their quantum efficiencies are determined, which indicates that the different hybrid material systems derived from different functionalized calix[4]arene bridges present different luminescence behavior.

1. Introduction

Organic−inorganic hybrid materials have been widely studied in the past few years with their unique properties in many fields because they combine the advantages of both organic and inorganic parts.[1,2] According to the interaction among the different phases in hybrid systems, these hybrid materials can be mainly classified into two major classes: one is physically mixed with weak interactions (hydrogen bonding, van der Waals force, or weak static effect) between the organic and inorganic phases and the other is chemically bonded with chemical bonds.[3−6] The latter hybrids belong to the molecular-based systems, which can realize the possibility of tailoring complementary properties of novel multifunctional advanced materials through chemical bonding within different components in a single material.[7] As for the preparation of such hybrid materials, the sol−gel technique has proven to be a convenient synthetic method because of its unique characteristics, namely, low temperature and versatility.[8] Rare-earth ions are famous for their unique luminescence properties characterized by a broad spectral range (from ultraviolet to IR regions) and, in particular, a strong narrow-width emission band in the visible region, a wide range of lifetimes that are suitable for various applications. Rare-earth-containing hybrid materials have attracted attention for optical applications owing to their excellent luminescence characteristics from electronic transitions

* To whom correspondence should be addressed. E-mail: byan@tongji.edu.cn. Phone: +86-21-65984663. Fax: +86-21-65982287.
† Tongji University.
‡ Peking University.

(1) Suratwala, T.; Gardlund, Z.; Davidson, K.; Uhlmann, D. R.; Watson, J.; Peyghambarian, N. *Chem. Mater.* **1998**, *10*, 190.
(2) Molina, C.; Dahmouchue, K.; Santilli, C. V.; Craievich, A. F.; Ribeiro, S. J. L. *Chem. Mater.* **2001**, *13*, 2818.
(3) Harreld, J. H.; Esaki, A.; Stucky, G. D. *Chem. Mater.* **2003**, *15*, 3481.
(4) Minoofar, P. N.; Hernandez, R.; Chia, S.; Dunn, B.; Zink, J. I.; Franville, A. C. *J. Am. Chem. Soc.* **2002**, *124*, 14388.
(5) Choi, J.; Tamaki, R.; Kim, S. G.; Laine, R. M. *Chem. Mater.* **2003**, *15*, 3365.
(6) Dong, D. W.; Jiang, S. C.; Men, Y. F.; Ji, X. L.; Jiang, B. Z. *Adv. Mater.* **2000**, *12*, 646.
(7) Kawa, M.; Frechet, J. M. J. *Chem. Mater.* **1998**, *10*, 286.
(8) Sanchez, C.; Ribot, F. *New J. Chem.* **1994**, *18*, 1007.

10.1021/ic801465p CCC: $40.75
Published on Web 04/06/2009

between the 4f energy levels.[9,10] Much previous work has been done on physical mixing methods. Embedding rare-earth complexes with aromatic carboxylic acid, β-diketone, or heterocyclic ligands in a sol−gel-derived matrix has been described in many studies. However, these hybrid materials have many disadvantages such as the dopant concentration of a complex silica matrix is very low and it is hard to obtain transparent and uniform material. Poor mechanical properties also restrict its practical application.[11−13] The present work focuses on the latter hybrid system with rare-earth-complex luminescent centers bonded with a siloxane matrix through Si−O linkages.[14−20]

Our recent work concerns the covalently bonded hybrids.[21−28] We have successfully realized five paths to construct rare-earth hybrid materials with chemical bonds, such as the amino group modification path,[21,22] carbonyl group modification path,[23,24] hydroxyl group modification path,[25,26] methyl group extraction path,[27] and sulfonamide bridge path.[28] In view of these researches, it can be recognized that the key procedure to construct molecular-based materials is to design a "functional bridge molecule" by a grafting reaction, which can perform the double function of both coordinating rare-earth ions and processing sol−gels to constitute a covalent Si−O network.[20−28] The development of novel linkages for connecting organic compounds to inorganic solid supports is an important and active area because the choice of the linker is a key consideration in designing a material because the stability of the linker limits the chemistry in the synthesis route and the final materials' properties.[20−28]

We have explored this hypothesis through the synthesis of calix[4]arene derivatives in which the functional group contains a silicon alkoxide group suitable for hydrolysis and polymerization to form a Si−O network. In fact, the calixarene-modified silica gel has been applied to the functional material in analytical chemistry, especially in a chromatogram.[29,30] Besides the ordered, mesoporous inorganic/organic hybrid polymers containing covalently and multiply bound microporous organic hosts such as a calixarene derivative,[31] the mesoporous silica functionalized by a covalently bound calixarene-based fluoroionophore for selective optical sensing of mercury(II) in water can be obtained.[32] On the other hand, the calixarene can also be used to modify the silica to coat the optical semiconductor nanoparticle.[33,34] Because it is known that the calixarene chromophore can absorb light strongly, transfer excitation efficiently to rare-earth ions, and protect ions from interactions that provide a quenching pathway,[35,36] it is our hope to introduce the complex of rare-earth ions with a calixarene derivative to a silicon skeleton, which may provide a subtle way of controlling the luminescence properties. The mode of functionalization is chosen to be the same as that widely explored elsewhere,[37−40] in the hope that the complex may possess excellent light-conversion properties such as that widely explored previously. In this paper, two novel kinds of organic ligand precursors, *p-tert*-butylcalix[4]arene and calix[4]arene, are chosen as molecular precursors, which can react with 3-(triethoxysilyl)propyl isocyanate (TESPIC).[41] Then these multifunctional organosilane precursors are submitted to a complex with Eu^{3+}/Tb^{3+} ions and to a sol−gel process in order to obtain the anticipated hybrid materials. Here we design a molar ratio of 1:1 for a calixarene precursor and TESPIC, for which it is considered to be easy to control the reaction than other molar ratio.[37] Reactions are generally performed at room temperature, where gelation particles have to be stabilized by chemical cross-linking. As an alternative, we developed an oil-in-water emulsion process involving the drying of gelation particles on a vacuum line, followed by the rapid condensation of silicates, leading to stable hybrid microparticles. The structure of the deposited silica particles appears to depend on both the organosilane concentration and the coordination interactions. In this way, numerous calixarenes and their derivatives are expected to be introduced into the hybrids and more multifunctional luminescent materials could be obtained.

(9) Corriu, R. J. P.; Leclercq, D. *Angew. Chem., Int. Ed. Engl.* **1996**, *35*, 1420.
(10) Hufner, S. *Optical spectra of transparent rare earth compounds*; Academic Press: New York, 1978.
(11) Murtagh, M. T.; Kwon, H. C.; Shahriari, M. R.; Krihak, M.; Ackley, D. E. *J. Mater. Res.* **1998**, *13*, 3326.
(12) Tanner, P. A.; Yan, B.; Zhang, H. J. *J. Mater. Sci.* **2000**, *35*, 4325.
(13) Gracia, J.; Mondragon, M. A.; Tellez, C.; Campero, A.; Castano, V. M. *Mater. Chem. Phys.* **1995**, *41*, 15.
(14) Wang, F. F.; Yan, B. *J. Organomet. Chem.* **2007**, *692*, 2395.
(15) Yan, B.; Qiao, X. F. *J. Phys. Chem. B* **2007**, *111*, 12362.
(16) Li, Y.; Yan, B.; Yang, H. *J. Phys. Chem. C* **2008**, *112*, 3959.
(17) Sanchez, C.; Lebeau, B.; Chaput, F.; Boilot, J. P. *Adv. Mater.* **2003**, *15*, 1969.
(18) Moreau, J. J. E.; Vellutim, L.; Man, M. W. C.; Bied, C.; Bantignles, J. *J. Am. Chem. Soc.* **2001**, *123*, 1509.
(19) Moreau, J. J. E.; Vellutim, L.; Man, M. W. C.; Bied, C.; Bantignles, J. L.; Dieudonne, P.; Sauvajol, J. L. *J. Am. Chem. Soc.* **2001**, *123*, 7957.
(20) Cerveau, G.; Corriu, R. J. P.; Framery, E.; Lerouge, F. *Chem. Mater.* **2004**, *16*, 3794.
(21) Wang, Q. M.; Yan, B. *J. Mater. Chem.* **2004**, *14*, 2450.
(22) Wang, Q. M.; Yan, B. *J. Photochem. Photobiol. A: Chem.* **2006**, *178*, 70.
(23) Wang, Q. M.; Yan, B. *Cryst. Growth Des.* **2005**, *5*, 497.
(24) Wang, Q. M.; Yan, B. *J. Photochem. Photobiol. A: Chem.* **2006**, *175*, 159.
(25) Wang, Q. M.; Yan, B. *J. Organomet. Chem.* **2006**, *691*, 3567.
(26) Liu, J. L.; Yan, B. *J. Phys. Chem. C* **2006**, *112*, 14168.
(27) Yan, B.; Wang, Q. M. *Cryst. Growth Des.* **2008**, *8*, 1484.
(28) Yan, B.; Lu, H. F. *Inorg. Chem.* **2008**, *47*, 5601.
(29) Katz, A.; Da Costa, P.; Lam, A. C. P.; Notestein, J. M. *Chem. Mater.* **2002**, *14*, 3364.
(30) Liu, M.; Li, L. S.; Da, S. L.; Feng, Y. Q. *Talanta* **2005**, *66*, 479.
(31) Liu, C. Q.; Lambert, J. B.; Fu, L. *J. Am. Chem. Soc.* **2003**, *125*, 6452.
(32) Metivier, R.; Leray, I.; Lebeau, B.; Valeur, B. *J. Mater. Chem.* **2005**, *15*, 2965.
(33) Li, H. B.; Qu, F. G. *J. Mater. Chem.* **2007**, *17*, 3536.
(34) Li, H. B.; Qu, F. G. *Chem. Mater.* **2007**, *19*, 4148.
(35) Bunzli, J. G.; Froidevaux, P.; Piguet, C. *Adv. Mater. Res.* **1994**, *1*, 1.
(36) Sabbatini, N.; Guardigli, M.; Lehn, J. *Coord. Chem. Rev.* **1993**, *123*, 201.
(37) Yan, B.; Wang, Q. M.; Ma, D. J. *Inorg. Chem.* **2009**, *48*, 36.
(38) Danil de Namor, A. F.; Jafou, O. *J. Phys. Chem. B* **2001**, *105*, 8018.
(39) Froidevaux, P.; Harrowfield, J. M.; Sobolev, A. N. *Inorg. Chem.* **2000**, *39*, 4678.
(40) Oueslati, I.; Ferreira, R. A. S.; Carlos, L. D.; Baleizo, C.; Berberan-Santos, M. N.; de Castro, B.; Vicens, J.; Pischel, U. *Inorg. Chem.* **2006**, *45*, 2652.
(41) Yakovenko, A. V.; Boyko, V. I.; Kushnir, O. V.; Tsymbal, I. F.; Lipkowski, J.; Shivanyuk, A.; Kalchenko, V. I. *Org. Lett.* **2004**, *6*, 2769.

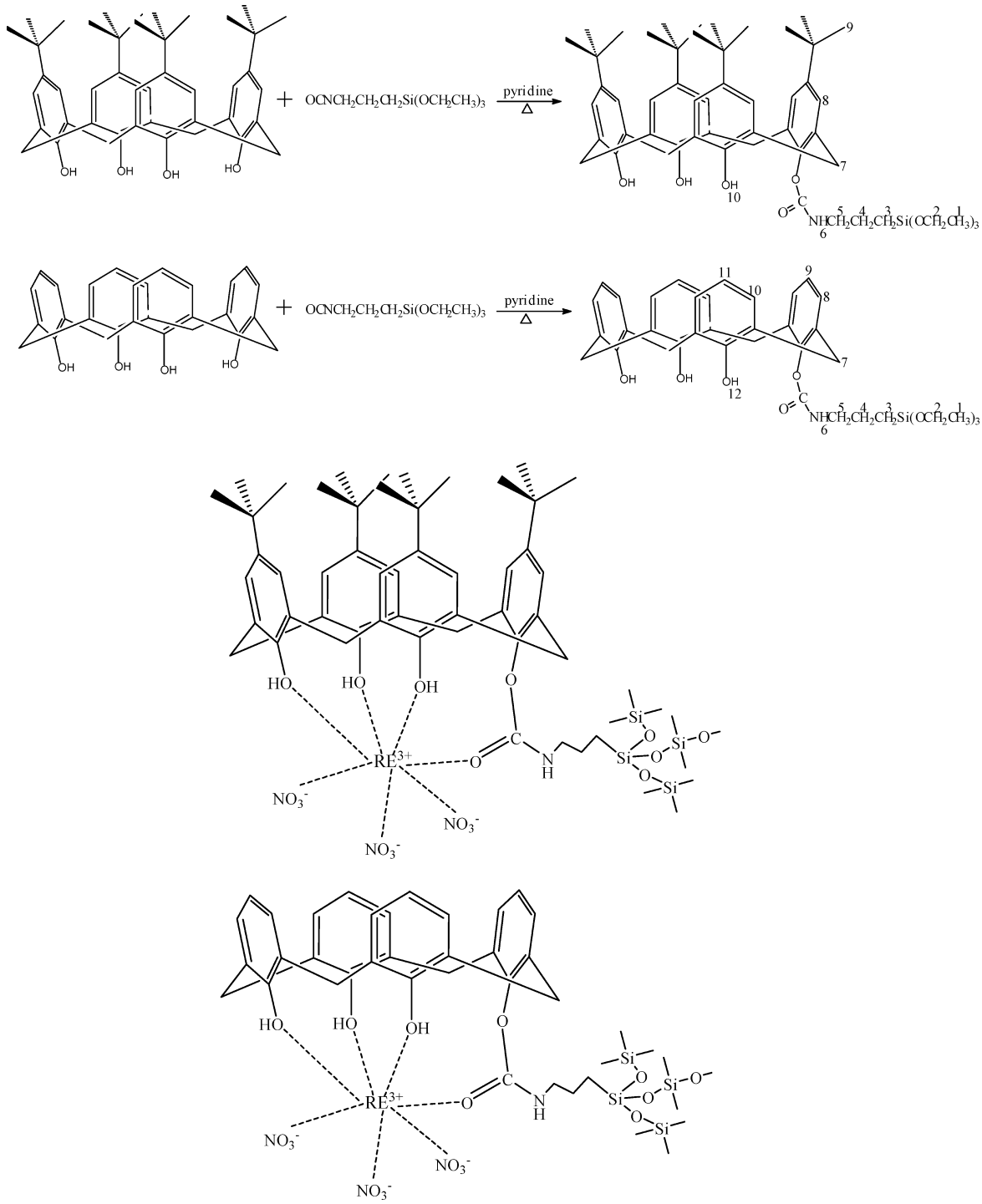

Figure 1. Scheme of typical procedures for the preparation of hybrid precursors and materials: (A) *p-tert*-butylcalix[4]arene systems; (B) calix[4]arene systems.

2. Experimental Section

2.1. Chemicals and Procedures. Starting materials were purchased from Alfa Ltd. and were used as received. All normal organic solvents were purchased from China National Medicines Group and were distilled before utilization according to literature procedures.[42] Terbium and europium nitrates were obtained from their corresponding oxides in dilute nitric acid.

2.2. Synthesis of Macrocyclic Precursor Linkages. The typical procedure for the preparation of hybrid precursor BC[4]Si (C[4]Si) is described in Figure 1. To a solution of 0.1944 g (0.3 mmol) of *p-tert*-butylcalix[4]arene (0.1272 g (0.3 mmol) of calix[4]arene) in 20 mL of pyridine was added dropwise with stirring 0.0742 g (0.3 mmol) of 3-(triethoxysilyl)propyl isocyanate (TESPIC) dissolved in 5 mL of pyridine. The mixed solution was warmed at 60 °C overnight. When the reaction was complete, the solvent was removed in vacuo, and a residue was obtained and then recrystallized by toluene, yielding 0.113 g (42.1%) [C[4]Si: 0.091 g (45.3%)]. Elem anal. Calcd for BC[4]Si, $C_{54}H_{77}NSiO_8$: C, 72.40; H, 8.60; N, 1.56. Found: C, 72.11; H, 8.33; N, 1.47. Elem anal. Calcd for C[4]Si, $C_{38}H_{45}NSiO_8$: C, 67.96; H, 6.71; N, 2.09. Found: C, 68.41; H, 6.42; N, 1.97. ^{1}H NMR for BC[4]Si ($CDC1_3$, 500

(42) Perrin, D. D.; Armarego, W. L. F.; Perrin, D. R. *Purification of Laboratory Chemicals*; Pergamon Press: Oxford, U.K., 1980.

MHz): δ 0.64 (t, 2H, H_3), 1.22 (t, 9H, H_1), 1.22 (s, 36H, H_{10}), 1.62 (m, 2H, H_4), 3.15 (m, 2H, H_5), 3.82 (q, 6H, H_2), 4.25 (m, 8H, H_7), 4.55 (s, 1H, H_6), 7.02 (s, 6H, H_9), 7.25 (s, 2H, H_8), 10.35 (s, 3H, H_{11}). ^{1}H NMR for C[4]Si ($CDC1_3$, 500 MHz): δ 0.68 (t, 2H, H_3), 1.24 (t, 9H, H_1), 1.70 (m, 2H, H_4), 3.26 (m, 2H, H_5), 3.80 (q, 6H, H_2), 4.22 (m, 8H, H_7), 4.55 (s, 1H, H_6), 6.72 (t, 3H, H_{11}), 7.05 (d, 6H, H_{10}), 7.25 (t, 1H, H_9), 7.32 (d, 2H, H_8), 10.18 (s, 3H, H_{12}).

2.3. Preparation of Hybrid Systems. Preparation of BC[4]-Si and C[4]-Si. The sol−gel-derived hybrid was prepared as follows: 0.2 mmol of a hybrid precursor and 0.4 mmol of tetraethoxysilane (TEOS) were dissolved in 5 mL of absolute ethanol with stirring. The mixture was kept warm and agitated magnetically to achieve a single phase in a covered Teflon beaker for 4 h, and then 30 mL of water was added under gentle magnetic stirring for 1 h. After that, it was dried on a vacuum line at 60 °C for about 6 days until the sample solidified. The obtained molecular hybrid material was collected as monolithic gels, then washed with ethanol, and dried at 80 °C for about 2 days. The final gels were ground into a powdered material for physical property studies (see Figure 1).

Preparation of RE-BC[4]Si and RE-C[4]Si. The sol−gel-derived hybrid containing rare-earth ions was prepared as follows: 0.2 mmol of a precursor was dissolved in 5 mL of ethanol. Then 0.2 mmol of $RE(NO_3)_3 \cdot 6H_2O$ ($Tb(NO_3)_3 \cdot 6H_2O$ and $Eu(NO_3)_3 \cdot 6H_2O$) was added into the solution, respectively. The resulting mixture was kept warm for about 5 h with stirring until the coordination reaction was accomplished. After that, 0.2 mmol of TEOS was added. The mixture was agitated magnetically to achieve a single phase for 4 h, and then 30 mL of water was added under gentle magnetic stirring for 1 h. The hybrid material was collected as monolithic gels, then washed with ethanol, and dried at 80 °C for about 2 days. The final gels were ground into a powdered material for physical property studies (see Figure 1).

2.4. Physical Measurements. Fourier transform infrared (FTIR) spectra were measured within the 4000−400 cm^{-1} region on a Nicolet model 5SXC IR spectrophotometer with the KBr pellet technique. ^{1}H NMR (proton nuclear magnetic resonance) spectra were recorded in $CDCl_3$ on a Bruker Avance-500 spectrometer with tetramethylsilane as the internal reference. Elemental analyses (C, H, and N) were determined with an Elementar Cario EL elemental analyzer. The X-ray diffraction (XRD) measurements were carried out on powdered samples via a "Bruker D8" diffractometer (40 mA and 40 kV) using monochromated Cu Kα_1 radiation (λ = 1.54 Å) over the 2θ range of 10−70°. Reflectivity spectra were recorded on a Bws003 spectrometer equipped with a diffuse-reflectance accessory. Phosphorescent spectra (chloroform solution) and luminescence (excitation and emission) spectra of these solid complexes were determined with a RF-5301 spectrophotometer whose excitation and emission slits were 5 and 3 nm, respectively (resolution, 0.05 nm; wavelength precision, ±0.2 nm; wavelength repetition, ±0.1 nm). Luminescent lifetimes were recorded on an Edinburgh FLS 920 phosphorimeter using a 450 W xenon lamp as the excitation source (pulse width, 3 μs). The outer luminescent quantum efficiency was determined using an integrating sphere (150 mm diameter, $BaSO_4$ coating) from an Edinburgh FLS920 phosphorimeter. The quantum yield can be defined as the integrated intensity of the luminescence signal divided by the integrated intensity of the absorption signal. The absorption intensity was calculated by subtracting the integrated intensity of the light source with the sample in the integrating sphere from the integrated intensity of the light source with a blank sample in the integrating sphere. All of the above measurements were completed at room temperature. Thermogravimetry was obtained on a Netzsch model STA 409C under the following conditions: atmosphere of oxygen air, heating/cooling rate of 10 °C/min, 18.78 mg of powder, and crucibles of Al_2O_3. Scanning electron microscopy (SEM) images were obtained on a Philips XL30 microscope.

3. Results and Discussion

3.1. Physical Characterization of Hybrid Materials. As detailed in the Experimental Section, elemental analysis and the ^{1}H NMR spectra relative to the macrocyclic precursor linkages were in full agreement with the proposed structure. The ^{1}H NMR chemical shifts relative to −CONH− groups observed in BC[4]Si (C[4]Si) can demonstrate the completion of the grafting reaction between *p-tert*-butylcalix[4]arene (calix[4]arene) and TESPIC. Besides, the multiple splitting of the ^{1}H NMR signal of the hydrogens numbered 5 and 7 can further indicate the occurrence of the hydrogen-transfer reaction. Integration of the ^{1}H NMR signals corresponding to ethoxy groups shows that no hydrolysis of the precursors occurred during the grafting reaction.

IR Spectra of Macrocylic Precursors and Hybrid Materials. The FTIR spectra for BC[4] (a), the precursor BC[4]Si (b), hybrid BC[4]Si (c), and Eu-BC[4]Si (d) are shown in Figure 2A, and the FTIR spectra of C[4] (a), the precursor C[4]Si (b), hybrid C[4]Si (c), and Eu-C[4]Si (d) are shown in Figure 2B. From BC[4] (a) to the precursor BC[4]Si (b), the modification is proven by the appearance of the peak at 1647 cm^{-1}, which is the unique vibration of the C═O group;[43] meanwhile, no absorption band characteristic of the ν(N═C═O) vibration originating from TESPIC was detected at 2277 cm^{-1}, which is further proof of completion of the reaction. In the spectra of the precursor (b), the presence of the ν(Si−C) absorption, which is located at 1200 cm^{-1} wavelength, is consistent with the fact that no Si−C bond cleavage occurs.[44] In the spectra of hybrid materials (BC[4]Si (c) and Eu-BC[4]Si), the spectra are dominated by the ν(Si−O−Si) absorption bands at around 1078 cm^{-1} wavelength, which can indicate the formation of siloxane bonds during hydrolysis/condensation reactions.[42] However, the ν(O−H) vibration at around 3400 cm^{-1} can also be obviously observed, which means the existence of residual silanol groups and the presence of a H_2O molecule. The coordination between rare-earth ions and the ligands can also be clearly shown by IR spectroscopy. In the spectrum of BC[4]Si (a), the ν (C−O−H) vibration is located at 1368 cm^{-1} and is medium intensity. However, in the spectrum of Eu-BC[4]Si (d), the ν(C−O−H) vibration is shifted to 1386 cm^{-1} and shifts to strong intensity. The shift is proof of the coordination of the phenolic group to the metallic ion with the oxygen atoms.[44] Furthermore, the ν(C═O) vibrations in Eu-BC[4]Si (d) are shifted to lower frequency (from 1647 cm^{-1} in BC[4]Si to 1625 cm^{-1}, $\Delta\nu$ = 22 cm^{-1}). This is ascribe to the complexation of the RE^{3+} ion with the oxygen

(43) Pretsch, E.; Buhlmann, P.; Affolter, C. *Structure Determination of Organic Compounds*, 2nd printing; Springer: Berlin, 2003.
(44) Franville, A. C.; Zambon, D.; Mahiou, R. *Chem. Mater.* **2000**, *12*, 428.

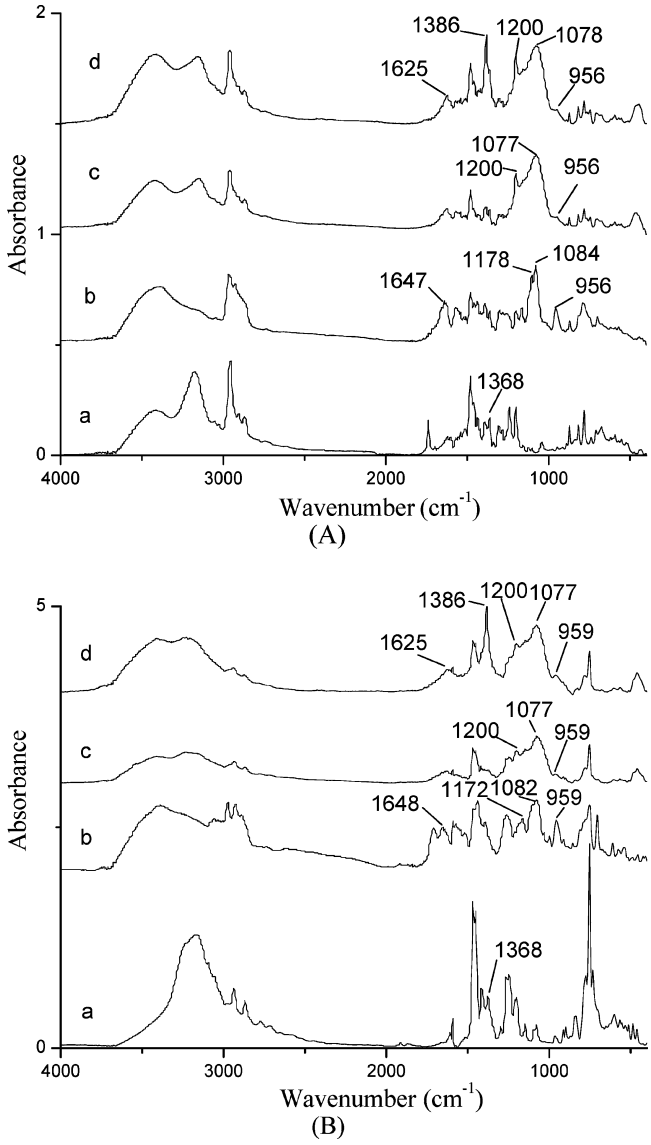

Figure 2. IR spectra of calixarene (a), the precursor of modified calixarene (b), hybrid materials without rare-earth ions (c), and hybrid materials with terbium ions (d): (A) *p-tert*-butylcalix[4]arene systems; (B) calix[4]arene systems.

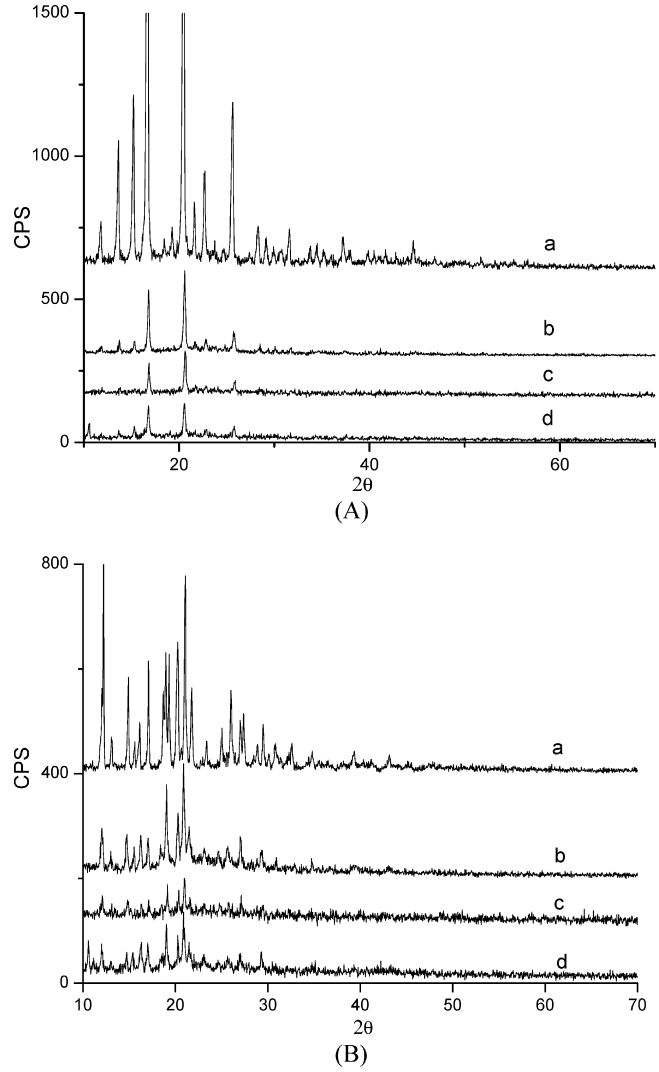

Figure 3. Selected XRD graphs of calixarene (a), the precursor of modified calixarene (b), hybrid materials without rare-earth ions (c), and hybrid materials with terbium ions (d): (A) *p-tert*-butylcalix[4]arene systems; (B) calix[4]arene systems.

atom of the C═O group in hybrids.[43] Besides, the stretching vibration of the nitrate ion [$\nu(NO_3^-)$], which is located at about 1377 cm^{-1}, can also be observed in the spectra of Eu-BC[4]Si (d). This indicates that the nitrate ion may coordinate with the rare-earth ions in the hybrid systems. Likewise, the FTIR spectra of C[4] (a), the precursor C[4]Si (b), hybrid C[4]Si (c), and Eu-C[4]Si (d) present features similar to those of Figure 2A for the above BC[4] hybrid systems.

XRD Patterns. XRD graphs are compared to study calix[4]arene derivatives and their corresponding hybrid materials. Figure 3A shows XRD graphs for hybrid systems of *p-tert*-butylcalix[4]arene. In the spectrum of *p-tert*-butylcalix[4]arene (a), there are characteristic XRD peaks of *p-tert*-butylcalix[4]arene crystals. However, the diffractogram of hybrid materials reveals that all of the hybrid materials with $10° \leq n \leq 70°$ are mostly amorphous while the intensities of the *p-tert*-butylcalix-[4]arene group XRD peaks decrease. This may be ascribed to the fact that the regular arrangement of the organic *p-tert*-butylcalix[4]arene group was disturbed by the introduction of the siliceous skeleton. Furthermore, the formation of the Si−O−Si matrixes through the hydrolysis/polycondensation process can largely influence the disorder of the organization of the organic ingredient; the presence of organic chains in the host inorganic framework resulted the absence of crystalline regions in these samples. So, in a comparison of hybrid material (c) with hybrid material (b), the material is more amorphous and the intensity of the *p-tert*-butylcalix[4]arene group decreases more. However, as for (b) and (d), the intensities of the narrow peaks are similar. It seems that the introduction of the rare-earth ions has no influence on the disorder structure of the siliceous skeleton. In addition, none of the hybrid materials contains measurable amounts of phases corresponding to the free rare-earth nitrate, which is an initial indication for the formation of the true covalent-bonded molecular luminescent hybrid materials.

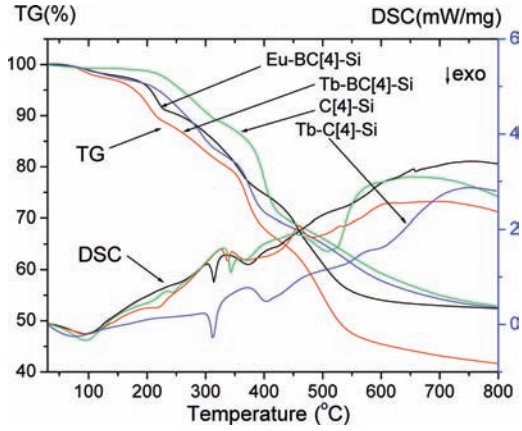

Figure 4. Selected DSC and TGA traces of Eu-BC[4]Si, Tb-BC[4]Si, C[4]Si, and Tb-C[4]Si hybrid materials.

The XRD graphs for hybrid systems of calix[4]arene present similar fetures (Figure 3B).

TGA−DSC Characterization of Hybrid Materials. Thermogravimetric analysis (TGA) and differential scanning calorimetry (DSC) were performed to examine the thermal activities of the hybrid materials. Figure 4 shows the TGA and DSC traces of the hybrids Eu-BC[4]Si, Tb-BC[4]Si, C[4]Si, and Tb-C[4]Si. From the curves, we can see that all of the samples show similar change trends in weight loss. The small weight loss between 50 and 180 °C was attributed to the desorption of physically absorbed or bonded water and the residuary solvent absolute ethanol, which is an endothermic process observed from the DSC curves. Compared with the TGA traces of C[4]Si and Tb-C[4]Si, the slight difference of the weight loss (about 1.2% for C[4]Si and 3.6% for Tb-C[4]Si) may be due to the amount of the coordinate H_2O molecule. It was calculated that there may be approximately one or two molecular H_2O molecules in each of the rare-earth ions. The weight loss between 180 and 550 °C was attributed to the thermal degradation of the organosilicate framework, involving Si−C, C−C, and C−N bond cleavage,[45] whereas the slight weight loss beyond 550 °C was ascribed to the release of H_2O formed from the further condensation of silanols in the silica framework. Because there even are some terminal Si−OH groups on the silica surface, these groups have the ability to undergo condensation to form Si−O−Si networks with an increase in the treatment temperature. Their slight differences of weight loss may be due to the different organic silylated precursors and the different degrees of polycondensation reaction. However, it seems that exchange of Eu^{3+} and Tb^{3+} ions has no influence on the thermal stabilities of the hybrids. This might be due to the fact that the structures of the siliceous skeleton were not changed. Likewise, the hybrid systems present similar results. Compared with the pure organic complexes, the thermal stabilities of these kinds of materials were improved; this may be due to the rigid silica matrix surrounding the organic complexes by molecular level hybridization.[46−48]

SEM Images of Hybrid Materials. The SEM images of the hybrids without RE^{3+} (Figure 5a for BC[4]Si; Figure 5b for C[4]Si) and the hybrids with RE^{3+} (Figure 5c for Eu-BC[4]Si; Figure 5d for Eu-C[4]Si; Figure 5e for Tb-BC[4]Si; Figure 5f for Tb-C[4]Si) can give some proof from the texture. For BC[4]Si and C[4]Si hybrids without rare-earth ions, the single hydrolysis and polycondensation reaction process very thoroughly without the outer interaction disturbed. Subsequently, the microparticle shows a small size of around 100−200 nm dimension. The micromorphology of the hybrids with europium or terbium ions seems to be largely different from those of BC[4]Si (or C[4]Si) despite the fact that they are prepared by the same process, forming some large spherelike micromorphology with 3−5 μm dimension. Because of the strong chelation effect between organic groups and rare-earth ions, the hydrolysis and polycondensation rate decrease. Besides, the organization may be induced under the chelation effect and other weak interactions such as van der Waals, London, and $\pi-\pi$ stacking.[18,19] The hybrid materials could be obtained through a polycondensation reaction between the terminal silanol groups of BC[4]Si (C[4]Si) and the OH groups of hydrolyzed TEOS. At the beginning of the reaction, the individual hydrolysis of BC[4]Si (C[4]Si) and TEOS is predominant. However, this is related to the polycondensation reactions between hydroxyl groups of both BC[4]Si (C[4]Si) and TEOS. By these methods, the covalently bonded hybrids BC[4]Si (C[4]Si) can be achieved. Similarly, the molecular-based composites bearing a RE−O coordination bond and Si−O covalent bonds can also be obtained after the introduction of RE^{3+}. In a comparison of BC[4]Si (C[4]Si) without RE^{3+} and RE-BC[4]Si (RE-C[4]Si) hybrids, an apparent distinction exists. The former only involves the sol−gel process (cohydrolysis and copolycondensation process), while in the latter a strong coordination reaction appears between RE^{3+} and BC[4]Si (C[4]Si), which have a great influence on the sol−gel process and the microstructure or physical properties of the hybrids. For BC[4]Si (C[4]Si) hybrids, the generous sol−gel process is favorable for mass transport, resulting in the smaller particle size of the microstructure. For RE-BC[4]Si (RE-C[4]Si) hybrids, when RE^{3+} (Eu^{3+} or Tb^{3+}) ions are introduced, the chelation effect between RE^{3+} and BC[4]Si (C[4]Si) naturally influences the hydrolysis and polycondensation process of BC[4]Si (C[4]Si) directly, furtherly influencing the growth tendency or the rate of the final hybrids, which can control their microstructure and luminescent properties. As we know, RE^{3+} possesses a high coordination number, so the chelated ability is strong and can play a role in the control of hybrids. Subsequently, coordination effects intervene the normal sol−gel process and limit the growth rate.

3.2. Photoluminescent Properties. Phosphorescence Spectra of Macrocylic Precursors. Phenolic group is already well-known to be a good chelating group to sensitize the luminescence of rare-earth ions. The mechanism is

(45) Tien, P.; Chau, L. K. *Chem. Mater.* **1999**, *11*, 2141.

(46) Yan, B.; Zhang, H. J.; Ni, J. Z. *J. Photochem. Photobiol. A: Chem.* **1998**, *112*, 231.

(47) Serra, O. A.; Nassa, E. I.; Zapparolli, G.; Rosa, I. L. V. *J. Lumin.* **1997**, *72*, 263.

(48) Shimojima, A.; Sugahara, Y.; Ohsuna, T.; Terasakl, O. *Nature (London)* **2002**, *416*, 304.

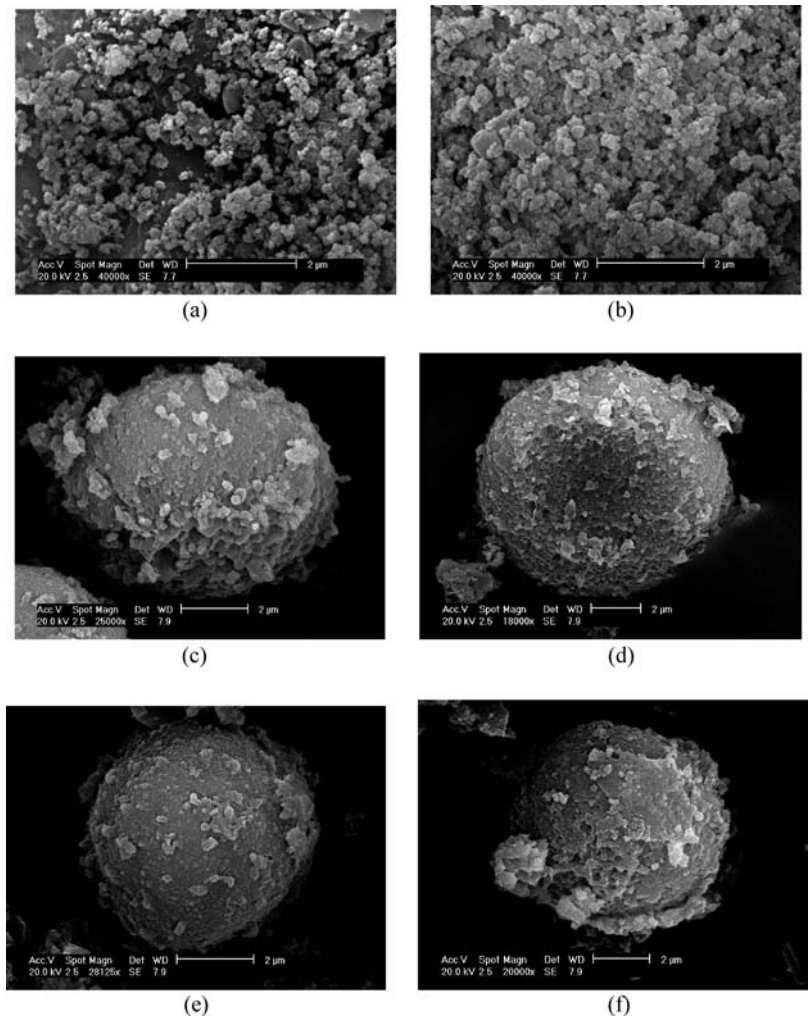

Figure 5. Selected SEM images for Eu-BC[4]Si, Tb-BC[4]Si, C[4]Si, and Tb-C[4]Si hybrid materials.

usually described as the antenna effect: the ligands reinforce the energy absorbability and transfer it to the metal ion with high efficiency. Then the emission from the rare-earth ions' excited state will be observed.[49] The phosphorescence spectra of BC[4] (a) and BC[4]Si (b) are recorded in Figure 6A. All of the curves exhibited a broad phosphorescence band, which corresponds to their triplet-state emission. A red shift was observed between BC[4] and precursor BC[4]Si because the modification of BC[4]Si enlarges the conjugation. The triplet-state energy is 24 272 cm^{-1} for BC[4] (a) and 22 883 cm^{-1} for BC[4]Si (b). The phosphorescence spectra of C[4] (a) and C[4]Si (b) are recorded in Figure 3B. A red shift also appeared between C[4] and C[4]Si for the graft silicone groups in C[4]Si to enrich the conjugation. The triplet-state energy is 23 420 cm^{-1} for C[4] (a) and 22 370 cm^{-1} for C[4]Si (b). The detailed phosphorescence data are given in Table 1. According to the energy-transfer and intramolecular energy mechanism,[50−53] the intramolecular energy migration efficiency from organic ligands to the central RE^{3+} is the most important factor determining the luminescence properties of rare-earth complexes.[50−53] So, there should exist an optimal energy difference between the triplet-state position of organic ligands and the emissive energy level of RE^{3+} ions; a larger value for the equation and a smaller value for the energy difference will decrease the luminescence properties of rare-earth complexes. As a consequence, the energy level differences between the triplet-state energies of both calix[4]arene (BC[4] or C[4]) and their molecular precursors (BC[4]Si or C[4]Si) are more suitable for the resonant emitting levels of Tb^{3+} (20 500 cm^{-1}) than Eu^{3+} (17 250 cm^{-1}), suggesting that the specific energy-transfer mechanism is more favorable for Tb^{3+} ions than Eu^{3+} ions. Besides, the modified molecular bridge (BC[4]Si or C[4]Si) has a better energy match to the luminescence of Tb^{3+} ions than Eu^{3+} ions for the triplet-state energy level decrease. The following emission spectra obtained from terbium and europium hybrids further demonstrate our predicted conclusion.

Photoluminescent Spectra. Parts a and b of Figure 7 show the selected excitation spectra of Tb-BC[4]Si and Tb-C[4]Si hybrids, respectively, both of which are monitored at 545 nm at room temperature. The spectra exhibit broad excitation

(49) Deacon, G. B.; Philips, R. J. *Coord. Chem. Rev.* **1980**, *33*, 227.
(50) Sato, S.; Wada, M. *Bull. Chem. Soc. Jpn.* **1970**, *43*, 1955.
(51) Dexter, D. L. *J. Chem. Phys.* **1953**, *21*, 836.
(52) Dean, C. R. S.; Shepherd, T. M. *J. Chem. Soc., Faraday Trans. II* **1975**, *71*, 146.
(53) Wang, Q. M.; Yan, B.; Zhang, X. H. *J. Photochem. Photobiol. A: Chem.* **2005**, *174*, 119.

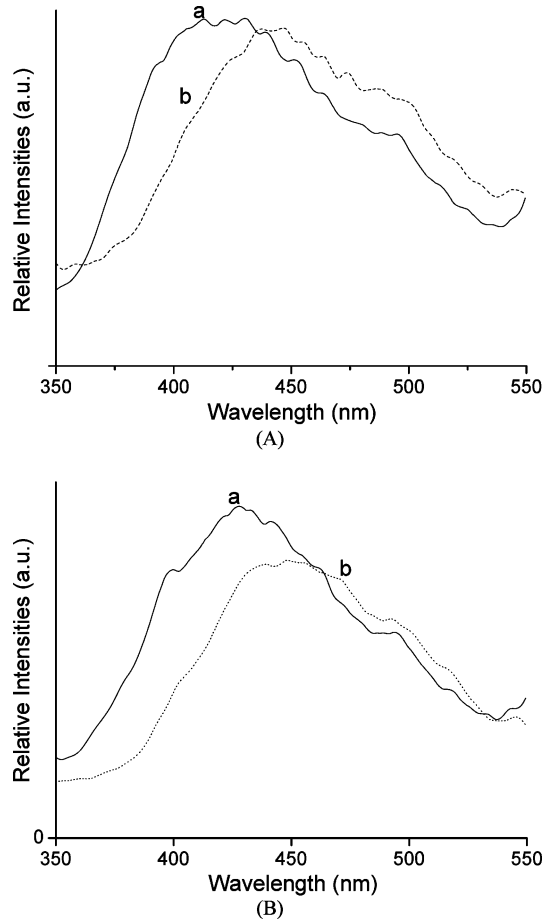

Figure 6. Phosphorescence spectra of calixarenes (a) and the precursor (modified calix[4]arenes) (b): *p-tert*-butylcalix[4]arene systems (A); calix[4]arene systems (B).

Table 1. Triplet-State Energies of Molecular Bridges and the Energy Transfer with Rare-Earth Ions

compound	λ_{max} (nm)	triplet-state energy (cm^{-1})	ΔE (Tr−Eu^{3+}) (cm^{-1})	ΔE (Tr−Tb^{3+}) (cm^{-1})
BC[4]	412	24 270	7020	3770
BC[4]Si	437	22 880	5630	2380
C[4]	427	23 420	6170	2920
C[4]Si	447	22 370	5120	1870

bands centered at 310 nm in the UV range, corresponding to the ligand-to-metal charge-transfer (CT) transition caused by interaction between the organic groups and the rare-earth

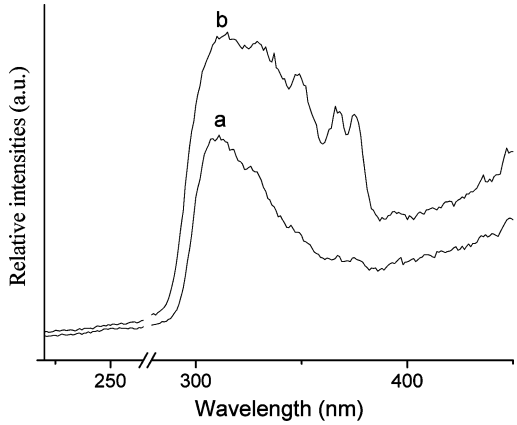

Figure 7. Selected excitation spectra of the resulting hybrid materials (a) Tb-BC[4]Si and (b) Tb-C[4]Si.

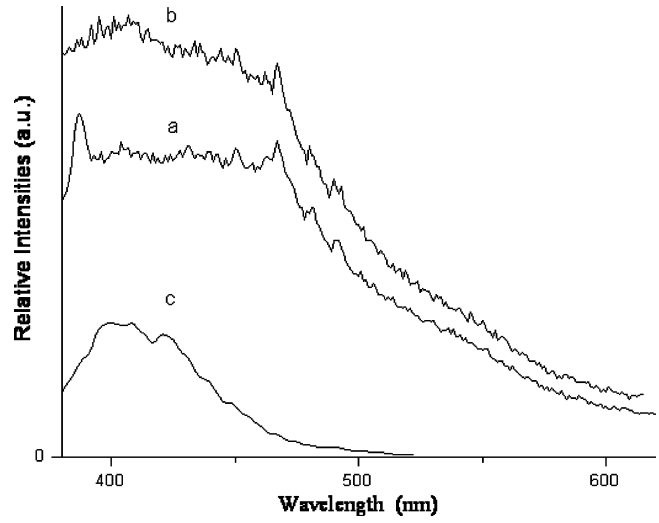

Figure 8. Emission spectra of hybrid materials: (a) BC[4]Si; (b) C[4]Si; (c) silica gel from TEOS (λ_{ex} = 295 nm).

ions.[54,55] No apparent f−f transitions could be observed in the spectra. The wide CT excitation bands will benefit the energy transfer and luminescence to terbium ions. Besides, the excitation spectrum of Tb-C[4]Si (Figure 7b) shows a broader band range and a stronger intensity than those of Tb-BC[4]Si (Figure 7a), which suggests that C[4]Si is a better energy match with Tb^{3+} than BC[4]Si.

Parts a and b of Figure 8 illustrate the typical centered blue-photoluminescence spectra of the BC[4]Si and C[4]Si hybrids, respectively. Because no rare-earth ions are introduced in them, these kinds of hybrid materials can only emit the luminescence of the organically modified Si−O network host with the much wider band range of over 150 nm across the violet−blue−green region, while for the emission spectrum of the pure Si−O network (SiO_2 silica gel from the hydrolysis and condensation process of TEOS), it merely shows the emission at the blue region with a band range of less than 100 nm. So, the two wide emission bands of BC[4]Si and C[4]Si hybrids suggest that the introduction of a macrocycle group enlarges the photoluminescent behavior effectively.

Figure 9 illustrates typical photoluminescence spectra of the terbium covalently bonded hybrid material. Narrow-width emission bands with maximum wavelengths at 487, 543, 580, and 621 nm are recorded. These bands are related to the transition from the triplet-state energy level of Tb^{3+} to the different single-state levels and are attributed to the $^5D_4 \rightarrow {}^7F_6$, $^5D_4 \rightarrow {}^7F_5$, and $^5D_4 \rightarrow {}^7F_4$ transitions of Tb^{3+} ions, respectively. The lower baseline in the spectra suggests that the energy-transfer efficiency between the organic groups and Tb^{3+} ions is higher than that between the organic groups and Eu^{3+} ions. Besides, the luminescent intensity of Tb-C[4]Si is slightly higher than that of Tb-BC[4]Si, suggesting that the energy match between C[4]Si and Tb^{3+} is more suitable than that between C[4]Si and Tb^{3+}. Further, we

(54) Binnemans, K.; Lenaerts, P.; Driesen, K.; Gorller-Walrand, C. *J. Mater. Chem.* **2004**, *14*, 191.
(55) Malta, O. L.; Brito, H. F.; Menezes, J. F. S.; Silva, F. R. G. E.; Alves, S.; Farias, F. S.; deAndrade, A. V. M. *J. Lumin.* **1997**, *75*, 255.

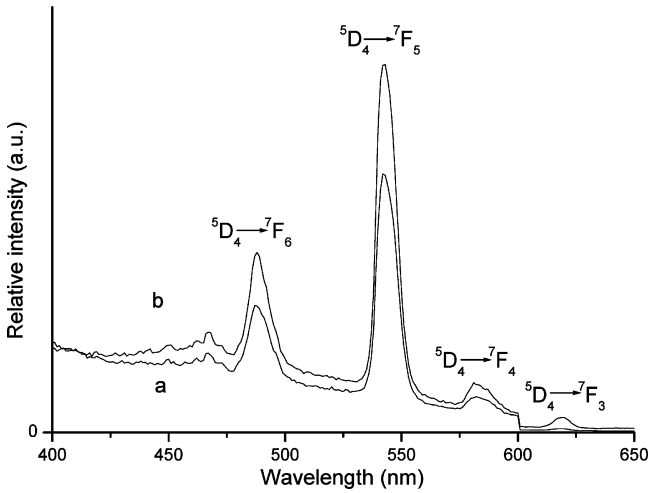

Figure 9. Emission spectra of the terbium hybrid materials: (a) Tb-BC[4]Si; (b) Tb-C[4]Si ($\lambda_{ex} = 310$ nm).

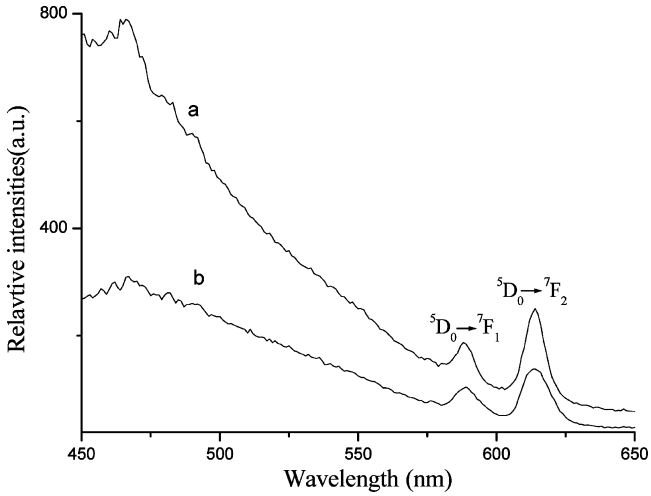

Figure 10. Emission spectra of the europium hybrid materials: (a) Eu-BC[4]Si; (b) Eu-C[4]Si ($\lambda_{ex} = 335$ nm).

selectively compared the luminescent spectra of the two terbium hybrids and the similar terbium-modified phenol sol−gel hybrids because they possess similar phenol hydroxyl groups and modified paths.[57] At the same measurement conditions, we found that both Tb-BC[4]Si and Tb-C[4]Si show higher luminescence intensity, suggesting that the introduction of a macrocycle of calix[4]arene is favorable for the energy-transfer and luminescence sensitization for Tb^{3+}.

Figure 10 illustrates typical photoluminescence spectra of europium hybrid materials. The maxima of these bands are at 590 and 613 nm, which are associated with $^5D_0 \rightarrow {}^7F_1$ and $^5D_0 \rightarrow {}^7F_2$ transitions, respectively. The energy transfer from the phenolic ligand to europium(III) is not perfect, as can be noticed by the residual ligand emission before 470 nm. This is not a surprise because the poor energy level match has been described in this paper previously. A prominent feature that may be noted in these spectra is the high intensity ratio of $I(^5D_0 \rightarrow {}^7F_2)/I(^5D_0 \rightarrow {}^7F_1)$. The intensity (the integration of the luminescent band) ratio of the $^5D_0 \rightarrow {}^7F_2$ transition to the $^5D_0 \rightarrow {}^7F_1$ transition has been widely used as an indicator of Eu^{3+} site symmetry.[56] When interactions of the rare-earth complex with its local chemical environment are stronger, the complex becomes more nonsymmetrical and the intensity of the electric−dipolar transitions becomes more intense. As a result, the $^5D_0 \rightarrow {}^7F_1$ transition (magnetic−dipolar transition) decreased and the $^5D_0 \rightarrow {}^7F_2$ transition (electric−dipolar transition) increased. In this situation, the intensity ratios are approximately 1.5. This ratio is only possible when the europium ion does not occupy a site with inversion symmetry.[57] It is clear that strong coordination interactions took place between the organic groups and rare-earth ions.

Table 2. Luminescence Data of the Covalently Bonded Hybrids

	BC[4]Si	C[4]Si	Tb-BC[4]Si	Tb-C[4]Si	Eu-BC[4]Si	Eu-C[4]Si
ν_{01} (cm^{-1})					17 007	16 978
ν_{02} (cm^{-1})					16 287	16 287
I_{02}/I_{01}					3.03	2.71
A_{01} (s^{-1})					50	50
A_{02} (s^{-1})					158	141
τ (μs)[a,b]	98	159	430[b]	355[b]	162[a]	186[a]
A_{rad} (s^{-1})					208	191
τ_{exp}^{-1} (s^{-1})					6173	5376
η_{ET} (%)			74	46	8.2	9.3
η (%)	14.8	16.1	10.7	6.9	1.3 (3.4)[c]	1.5 (3.6)[c]

[a] For the $^5D_0 \rightarrow {}^7F_2$ transition of Eu^{3+}. [b] For the $^5D_4 \rightarrow {}^7F_5$ transition of Tb^{3+}. [c] The calculated values in parentheses are from the spectra and lifetimes.

Luminescent Lifetimes, Quantum Efficiency, and Energy-Transfer Efficiencies. Typical decay curves of the europium and terbium hybrid materials were measured, and they can be described as a single exponential [$RE(S(t)/S_0) = -k_1t = -t/\tau$], indicating that all Eu^{3+} and Tb^{3+} ions occupy the same average coordination environment. The resulting lifetime data of europium and hybrids are given in Table 2. The luminescent lifetime of BC[4]Si is short than that of C[4]Si, suggesting that the introduction of a butyl group is not a benefit for the photoactivity of the whole calix[4]arene derivative. The luminescent lifetime of Tb-BC[4]Si (430 μs) is longer than that of Tb-C[4]Si (355 μs), while it is contrary to the luminescent lifetimes of Eu-BC[4]Si (162 μs) and Eu-C[4]Si (186 μs), which can be ascribed to the prediction from the energy match between BC[4]Si and C[4]Si and Eu^{3+} (Tb^{3+}) ions. Because the main energy donor in the hybrid systems originates from the photoactive BC[4]Si and C[4]Si functional groups, the energy match between the BC[4]Si and C[4]Si functional groups is the most important factor determining the luminescent lifetimes of the corresponding hybrid materials. The energy match between BC[4]Si and Eu^{3+} is more suitable than that between C[4]Si and Eu^{3+} because the energy difference $\Delta E(Tr-Eu^{3+})$ of BC[4]Si (2380 cm^{-1}) is better than that of C[4]Si (1870 cm^{-1}) according to the above discussion from the phosphorescence spectra. The energy difference of C[4]Si (1870 cm^{-1}) is too small to worsen the energy match, which easily produces the inverse energy loss to decrease the luminescent behavior. Similarly, the energy difference $\Delta E(Tr-Tb^{3+})$ of BC[4]Si (5630 cm^{-1}) is worse than that of C[4]Si (5120 cm^{-1}) and is so large that it decreases the energy transfer from the triplet state of BC[4]Si to Tb^{3+}, so the energy match between BC[4]Si and Eu^{3+} is less suitable

(56) Wang, Z.; Wang, J.; Zhang, H. J. *Mater. Chem. Phys.* **2004**, *87*, 44.
(57) Yan, B.; Ma, D. J. *J. Solid State Chem.* **2006**, *179*, 2059.

than that between C[4]Si and Eu^{3+}. Besides, the luminescent lifetimes of terbium hybrids are longer than those of europium hybrids, indicating that both BC[4]Si and C[4]Si are more suitable for the luminescence of Tb^{3+} than that for Eu^{3+}. So, the luminescent lifetime data for these rare-earth covalently bonded hybrids correspond to the above analyses from the phosphorescence spectrum. Besides, the luminescent lifetimes of Tb-BC[4]Si (430 μs) and Tb-C[4]Si (355 μs) are longer than those of terbium-modified phenol−silicon hybrids[52] (here we determined that it is 290 μs), which agrees with the results from the above luminescent intensity. The calixe[4]arene macrocycle enhances the photoluminescence behavior compared to the pure phenol derivative hybrids.

Further, we selectively determined the emission quantum efficiencies of the $^5D_0$ excited state of the europium ion for Eu^{3+} hybrids on the basis of the emission spectra and lifetimes of the $^5D_0$ emitting level; the detailed luminescent data are shown in Table 1. The quantum efficiency of the luminescence step, η, expresses how well the radiative processes (characterized by rate constant A_r) compete with the nonradiative processes (overall rate constant A_{nr}).[58−63]

$$\eta = A_r/(A_r + A_{nr}) \quad (1)$$

Nonradiative processes influence the experimental luminescence lifetime by the equation[58−63]

$$\tau_{exp} = (A_r + A_{nr})^{-1} \quad (2)$$

So, the quantum efficiency can be calculated from the radiative transition rate constant and experimental luminescence lifetime from the following equation:[58−63]

$$\eta = A_r\tau_{exp} \quad (3)$$

where A_r can be obtained by summing over the radiative rates A_{0J} for each $^5D_0 \rightarrow {}^7F_J$ transitions of Eu^{3+}.[58−63] The branching ratio for the $^5D_0 \rightarrow {}^7F_{5,6}$ transitions can be neglected because they both are not detected experimentally, the influence of which can be ignored in the depopulation of the $^5D_0$ excited state.[57−62] Because $^5D_0 \rightarrow {}^7F_1$ belongs to the isolated magnetic dipole transition, it is practically independent of the chemical environments around the Eu^{3+} ion and thus can be considered as an internal reference for the whole spectrum; the experimental coefficients of spontaneous emission, A_{0J} can be calculated according to the corrected luminescent spectra.[58−63] On the basis of the above discussion, the quantum efficiencies of the two kinds of europium hybrid materials can be determined in the order, which is lower than the value from the experimental measurement. This may be due to the fact that there exist some errors in the measurement and calculation of the spectra and lifetimes. In a comparison of the values of luminescent quantum efficiencies, it can be found that they show a rule similar to the value of luminescent lifetimes and correspond to the energy match between BC[4]Si and C[4]Si and Eu^{3+} (Tb^{3+}) ions. So, the different compositions of the hybrid materials may have an influence on the luminescent lifetimes and quantum efficiencies. Besides, it can be seen that the luminescent behavior for BC[4]Si shows no apparent distinction with that for other hybrids with different molar ratio.[37] On the basis of the data of luminescent quantum yields, it can also be predicted that the energy-transfer efficiencies from BC[4]Si and C[4]Si to Tb^{3+} are higher than those to Eu^{3+}. The experimental luminescent quantum efficiency and energy-transfer efficiency data verify the prediction.

4. Conclusions

In summary, two macrocycle ligands, *p-tert*-butylcalix[4]arene and calix[4]arene, have been functionalized by 3-(triethoxysilyl)propyl isocyanate through base-initiated nucleophilic addition and the two novel macrocyclic bridge molecules (abbreviated as BC[4]Si and C[4]Si) are engaged in the construction of three series of novel luminescent chemically bonded hybrid material systems (BC[4]Si, RE-BC[4]Si, C[4]Si, and RE-C[4]Si, where RE = Eu, Tb). It is found that the introduction of rare-earth ions (Eu^{3+}, Tb^{3+}) strongly affects the sol−gel organization and microstructure of the Si−O network from XRD and SEM. The energy match and intramolecular energy transfer between a functionalized calix[4]arene bridge and Eu^{3+} (Tb^{3+}) are studied, which mainly determine the luminescent behavior of the resulting molecular hybrids. These chemically bonded hybrids present blue (BC[4]Si and C[4]Si), green (Tb-BC[4]Si and Tb-C[4]Si), and red (Eu-BC[4]Si and Eu-C[4]Si) luminescence. The luminesent lifetimes and quantum efficiencies of these hybrids have been compared and discussed in detail, suggesting that the different hybrid material systems derived from different functionalized bridges present different luminescence efficiencies.

Acknowledgment. This work was supported by the National Natural Science Foundation of China (Grant 20671072) and the Program for New Century Excellent Talents in University.

IC801465P

(58) Werts, M. H. V.; Jukes, R. T. F.; Verhoeven, J. W. *Phys. Chem. Chem. Phys.* **2002**, *4*, 1542.
(59) Teotonio, E. E. S.; Espinola, J. G. P.; Brito, H. F.; Malta, O. L.; Oliveria, S. F.; de Faria, D. L. A.; Izumi, C. M. S. *Polyhedron* **2002**, *21*, 1837.
(60) Malta, O. L.; dos Santos, M. A. C.; Thompson, L. C.; Ito, N. K. *J. Lumin.* **1996**, *69*, 77.
(61) de Sa, G. F.; Malta, O. L.; Donega, C. D.; Simas, A. M.; Longo, R. L.; Santa-Cruz, P. A.; da Silva, E. F. *Coord. Chem. Rev.* **2000**, *196*, 165.
(62) Boyer, J. C.; Vetrone, F.; Capobianco, J. A.; Speghini, A.; Bettinelli, M. *J. Phys. Chem. B* **2004**, *108*, 20137.
(63) Reisfeld, R.; Jorgenson, C. K. In *Handbook on the Physics and Chemistry of Rare Earths*; Gschneider, K. A., Jr., Eyring, L., Eds.; Elsevier Science Publishers: Amsterdam, The Netherlands, 1987; Vol. 9, p 61.